Polycyclic aromatic hydrocarbons and black carbon in intertidal sediments of China coastal zones: Concentration…

6 authors, including:

Xiaofei Li
East China Normal University
33 PUBLICATIONS   162 CITATIONS

SEE PROFILE

Lijun Hou
East China Normal University
98 PUBLICATIONS   1,323 CITATIONS

SEE PROFILE

Ye Li
East China Normal University
20 PUBLICATIONS   120 CITATIONS

SEE PROFILE

Xianbiao Lin
East China Normal University
37 PUBLICATIONS   192 CITATIONS

SEE PROFILE

Some of the authors of this publication are also working on these related projects:

Project   nitorgen cycling View project

Project   PAHs research View project

Polycyclic aromatic hydrocarbons and black carbon in intertidal sediments of China coastal zones: Concentration, ecological risk, source and their relationship

Xiaofei Li [a,1], Lijun Hou [b,1], Ye Li [a], Min Liu [a,c,*], Xianbiao Lin [a], Lv Cheng [a]

[a] School of Geographical Sciences, East China Normal University, 3663 North Zhongshan Road, Shanghai 200062, China
[b] State Key Laboratory of Estuarine and Coastal Research, East China Normal University, 3663 North Zhongshan Road, Shanghai 200062, China
[c] Key Laboratory of Geographic Information Science, Ministry of Education, East China Normal University, 3663 North Zhongshan Road, Shanghai 200062, China

HIGHLIGHTS

- River runoffs were responsible for the high PAH pollution levels in the study area.
- BC and PAHs derived mainly from the combustion process of fossil fuels.
- BC was associated closely with the pyrolytic compounds of PAHs.
- Potential toxicity assessment of PAHs indicated low ecological risk in the study area.

GRAPHICAL ABSTRACT
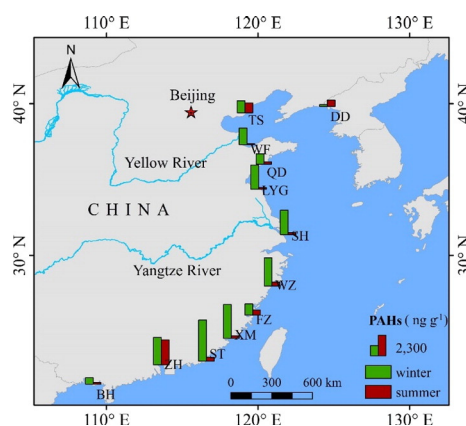
ABSTRACT

Polycyclic aromatic hydrocarbons (PAHs) and black carbon (BC) have attracted many attentions, especially in the coastal environments. In this study, spatiotemporal distributions of PAHs and BC, and the correlations between BC and PAHs were investigated in the intertidal sediments of China coastal zones. BC in sediments was measured through dichromate oxidation (BC_{Cr}) and thermal oxidation (BC_{CTO}). The concentrations of BC_{Cr} in the intertidal sediments ranged between 0.61 and 6.32 mg g^{-1}, while BC_{CTO} ranged between 0.57 and 4.76 mg g^{-1}. Spatial variations of $\delta^{13}C$ signatures in TOC and BC were observed, varying from −21.13‰ to −24.87‰ and from −23.53‰ to −16.78‰, respectively. PAH contents of sediments ranged from 195.9 to 4610.2 ng g^{-1} in winter and 98.2 to 2796.5 ng g^{-1} in summer, and significantly seasonal variations were observed at most sampling sites. However, the results of potential toxicity assessment indicated low ecological risk in the intertidal sediments of China coastal zones. Greater concentrations of PAHs measured in the sediments of estuarine environments indicated that rivers runoff may have been responsible for the higher PAH pollution levels in the intertidal sediments of China coastal zones. Pearson's correlation analysis suggested that pyrogenic compounds of PAH were significantly related to BC, due to that both BC and these compounds derived mainly from the combustion process of fossil

* Corresponding author at: Key Laboratory of Geographic Information Science, Ministry of Education, East China Normal University, 3663 North Zhongshan Road, Shanghai 200062, China.
  E-mail address: mliu@geo.ecnu.edu.cn (M. Liu).
[1] Contributed equally to this work.

Ecological risk
China coastal zones

fuels and biomass. Overall, increasing energy consumptions caused by anthropogenic activities can contribute more emissions of BC as well as PAHs and thus improve the importance of BC in indicating pyrogenic compounds of PAHs in the intertidal sediments of China coastal zones.

1. Introduction

Over the past few decades, extensive anthropogenic activities have resulted in the increasing emission of polycyclic aromatic hydrocarbons (PAHs) into the environments (Laflamme and Hites, 1978; Yunker et al., 1996; Liu et al., 2012a), thus causing unintentionally environmental issues on both regional and global scales (Zakaria et al., 2002; Liu et al., 2012a). Specifically, PAHs have been detected widely in various environment compartments including ambient atmosphere (Inomata et al., 2012), contaminated water (Wang et al., 2007), urban soils (Wang et al., 2014a), and coastal sediments (Liu et al., 2012a, 2012b). Likewise, the intertidal zones as the combinations of land and marine ecosystems receive substantial amount of PAHs, which may pose an ecological risk to coastal ecosystems (Countway et al., 2003; Moeckel et al., 2013). It is reported that the coastal sediments were polluted heavily by PAHs, especially in extensive anthropogenic activities coasts, and the PAHs derived mainly from burning of fossil fuels (Dudhagara et al., 2016). In addition, many studies reported that high concentrations of PAHs and associated high ecological risks were observed in coastal sediments (Savinov et al., 2003; Sprovieri et al., 2007; Chen et al., 2013). Therefore, increasing concerns regarding PAH pollution, ecological risk and sources in the sediments have been raised recently in coastal marine environments (Hung et al., 2007; Liu et al., 2012a, 2012b).

It has been reported that high molecular weight compounds of PAHs are primarily from pyrolytic origin such as combustion process of fossil fuels and biomass (Neff, 1979; Yunker et al., 2002). In addition to PAHs, a large amount of black carbon (BC) can also release into atmospheric environments (Wang et al., 2014b), and further transport into the sediments through atmosphere deposition and rivers runoff (Accardi-Dey and Gschwend, 2002; Koelmans et al., 2006; Agarwal and Bucheli, 2011; Liu et al., 2012a). Because pyrogenic compounds of PAHs are part of BC (Wiedemeier et al., 2015), their links have aroused many attentions (Oen et al., 2006; Sánchez-García et al., 2010). Thus, the BC may have potential importance in determining the fate of PAHs (pyrolytic compounds) in the coastal sediments (Koelmans et al., 2006; Agarwal and Bucheli, 2011). Furthermore, stable carbon isotope ratio (δ^{13}C) is an ideal tool to identify not only total organic carbon (TOC) sources (Peters et al., 1978), but also BC production pathways such as coal burning, internal engine and biomass combustion that can lead to distinct δ^{13}C values (McRae et al., 1999; Jautzy et al., 2013). Therefore, it is worth to reveal the distributions of BC and PAHs and the effects of both TOC and BC on pyrogenic compounds of PAHs in the intertidal sediments on a large space scale.

China, a higher energy consumption country, has experienced rapid economic development during the past three decades (Liu et al., 2012a). The contents of BC and PAHs thus increase dramatically in the environments as the results of extensive consumption of fossil fuels (Liu et al., 2012a; Wang et al., 2014b). It is estimated that annual riverine output and atmospheric outflow of PAHs in China were 367 and 8092 tons, respectively (Wang et al., 2007; Lang et al., 2008). However, China coastal zones are economically well developed and densely populated, which likely result in the release of great quantities of PAHs into the coastal environments (Liu et al., 2012a). Although previous studies have investigated the sources of PAHs in surface sediments of the coastal and marine environments (Guo et al., 2006; Liu et al., 2012a; Lin et al., 2011), no work has been done to reveal the fate and source of both BC and PAHs in intertidal sediments. Therefore, it is necessary to quantify spatial and temporal differences of BC and PAHs along China coastal zones.

The aims of the present study were to determine the spatiotemporal variations of PAHs and BC and identify the effects of both TOC and BC on PAHs in the intertidal sediments. In addition, the sources of PAHs in the intertidal sediments were identified. Ecological risk assessments of PAHs in the intertidal sediments were also performed based on toxic equivalents. This work provides new insights into the BC-derived PAHs in the intertidal sediments of China coastal zones.

2. Materials and methods

2.1. Sample collection

China's intertidal zones cover an area of 2.2×10^4 km^2, which is equivalent to 2.26% of China land area. China intertidal zones are of importance in providing extensive ecosystem services and biogeochemical cycles. In recent years, however, China intertidal zones have been suffered from degradation and polluted by various contaminants. Twelve sampling sites were selected, spanning from 21° 35.8′ N to 39° 55.2′ N along the coastal zones of China (Fig. 1). These sediment samples were collected in January (winter) and August seasons (summer) 2014, respectively. Three sampling plots of each sampling site were selected to account for small-scale sediment heterogeneity. At each sampling plot, surface sediment (0–5 cm depth) was collected with PVC tubes. After returning to laboratory, these core sediments were homogenized thoroughly under nitrogen gas condition and freeze-dried for the measurements of PAHs and BC.

In this study, five sampling sites are located in the estuaries, while the others are situated in the coasts (Fig. 1). Site DD is situated in Yalu River estuary, where is located in Dandong city, Liaoning Province. Site TS is situated in coastal zone of Tangshan city, Hebei Province. Site WF is situated in coastal zone of Weifang city, Shandong Province. Site QD is situated in coastal zone of QD city, Shandong Province. Site LYG is situated in coastal zone of Lianyungang city, Jiangsu Province. Site SH is situated in Yangtze estuary, where is located in Shanghai city. Site WZ is
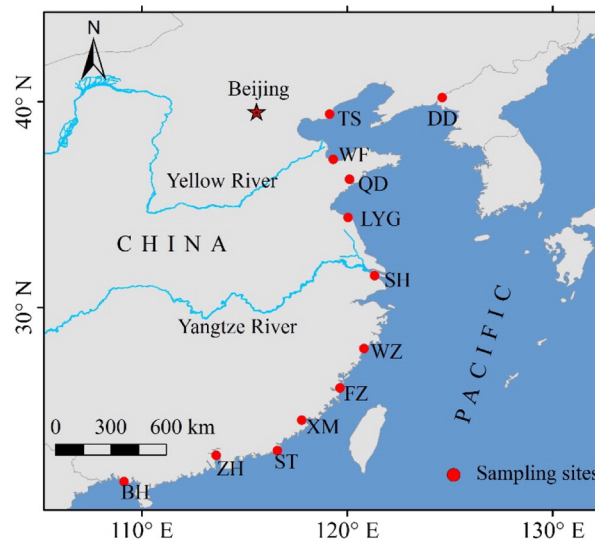

Fig. 1. Sampling sites along coastal regions of China. DD, TS, WF, QD, LYG, SH, WZ, FZ, XM, ST, ZH and BH are site abbreviations for Dandong, Tangshan, Weifang, Qingdao, Lianyungang, Shanghai, Wenzhou, Fuzhou, Xiamen, Shantou, Zhuhai and Beihai, respectively.

situated in Aojiang estuary, where is located in Wenzhou city, Zhejiang Province. Site FZ is situated in Minjiang estuary, where is in Fuzhou city, Fujian Province. Site XM is situated in Jiulongjiang estuary, where is in Xiamen city, Fujian Province. Site ST is situated in coastal zone of Shantou city, Guangdong Province. Site ZH is situated in Pearl River estuary, where is in Zhuhai city, Guangdong Province. Site BH is situated in coastal zone of Beihai city, Guangxi Province.

2.2. Total organic carbon and black carbon

Total organic carbon (TOC) of sediments were measured using a CHN elementary analyzer (Elementar analyzer vario Max CN, Germany) after removing carbonate with $1 \, mol \, l^{-1}$ HCl. BC in sediments was measured through chemical oxidation (dichromate oxidation, BC_{Cr}) and chemo-thermal oxidation (CTO-375, BC_{CTO}), respectively. The BC_{CTO} of sediments was determined by the chemo-thermal oxidation method based on the procedures reported by Gustafsson et al. (2001). In Brief, 2.0 g of sediment was leached by $1 \, mol \, l^{-1}$ HCl repeatedly to remove carbonate. Subsequently, the sediment was dried at 60 °C in an oven, and was then oxidized at 375 °C for 24 h. During the oxidation, the temperature ramp rate of oven was settled to be $2.5 \, °C \, min^{-1}$ to avoid potential artificial charring (Mitra et al., 2002). BC_{Cr} in sediments was measured using the methods reported by Lim and Cachier (1996) and Song et al. (2002) with slight modification. Briefly, 1.0 g of sediment was placed in a clean 50 ml centrifugal tube. After the sediment was wetted with deionized water, 2 ml of 1 M HCl was added into the tube twice at an interval of 1 h. The repeated twice acidifications were conducted to eliminate the carbonate completely. Subsequently, the wetted sediments were dried at 60 °C. The dried remains were spiked with $15 \, ml \, 0.1 \, mol \, l^{-1}$ of $K_2Cr_2O_7$: $2 \, mol \, l^{-1}$ of H_2SO_4 (1:1, v:v) and the reaction lasted 60 h at 55 °C. The $K_2Cr_2O_7$ was added to ensure the excess oxidation, and deionized water was also added a few times. In this study, the carbon contents after pretreatments of sediments were assumed the BC_{CTO} and BC_{Cr}, and thus were determined using a CHN elementary analyzer (Elementar analyzer vario Max CN, Germany).

2.3. Stable carbon isotop $\delta^{13}C(‰) = (R_{sample}/R_{reference} - 1) \times 1000e$ ratios analysis

Stable carbon isotope compositions ($\delta^{13}C$) of TOC and BC (BC_{CTO}) were determined by a Flash Elemental Analyzer (EA1112) connected to an Isotope Ratio Mass Spectrometer (Model: DELTA plus/XP, Finnigan MAT Co.). The stable carbon isotope compositions were expressed in δ notation as the deviation from standard reference material (‰) (Petrisic et al., 2013), where R_{sample} and $R_{reference}$ indicate heavy/light isotopic ratios (i.e. $^{13}C/^{12}C$) of the sample and reference, respectively. The $\delta^{13}C$ was given as ‰-deviation from the carbon isotope composition of the Vienna-Pee Dee Belemnite (PDB) standard. The analytical precision of the experiment processes was $\pm 0.2‰$ for $\delta^{13}C$ based on the replicate analysis of the same sample (Wu et al., 2013).

2.4. PAH extraction and analysis

The PAHs in sediment samples were extracted based on the U.S. EPA method (US EPA, 1996). Briefly, 2.5 g of sediment was Soxhlet-extracted with 120 ml of acetone/dichloromethane (1:1, v/v) for 24 h at 65 °C of water bath, after addition of deuterated PAH mixture standard solution ([$^2H_8$]naphthalene, [$^2H_{10}$]acenaphthene, [$^2H_{10}$]phenanthrene, [$^2H_{12}$]chrysene, and [$^2H_{12}$]perylene each at a concentration of $10 \, mg \, l^{-1}$) and activated copper powder. Subsequently, the extract was concentrated, solvent exchanged to hexane, and further concentrated before column fractionation with 1:2 (volume:volume) alumina/silica gel/anhydrous sodium sulfate (silica gel: activated at 130 °C for 12 h and deactivated with 10% Milli-Q water, alumina and anhydrous sodium sulfate: baked at 450 °C for 4 h and deactivated with 10% Milli-Q water). The first fraction eluted with 20 ml of hexane was discarded, while the second fraction including PAHs was eluted with 70 ml of hexane/dichloromethane, concentrated to 1.0 ml for analysis. The 16 EPA priority PAHs were measured using GC–MS equipped with a DB-5 polysiloxane polymer column (30 m × 250 μm × 0.25 μm) (Agilent 7890A/5975C). Further detailed information on instrumental analysis was summarized in the Supporting Information.

2.5. Quality control and quality assurance

The analysis procedures of PAHs were conducted through quality control and quality assurance as previously described by Zhang et al. (2012). The accuracy and precision of analyses for every 8 field samples were ensured through two blanks and standards (a mixture of 16 EPA PAHs and 5 deuterated PAHs). Furthermore, any background contamination was measured through method blanks. In addition, calibration standards were used to calibrate the instrument every day and differences between serial points calibrations and daily calibrations were <15%. The relative standard deviations were 2.1% and average deviations were 1.3% for each compound. The recoveries for surrogate standards for quality control of samples were in the range of 79.8–95.1, 79.9–95.7, 74.8–98.9, 77.8–106.2, and 80.1–101.7% for [$^2H_8$]naphthalene, [$^2H_{10}$]acenaphthene, [$^2H_{10}$]phenanthrene, [$^2H_{12}$]chrysene, [$^2H_{12}$]perylene, respectively. The limit of detection varied between $0.035 \, ng \, g^{-1}$ and $0.307 \, ng \, g^{-1}$, and the data measured was corrected.

2.6. Evaluation of toxicity and risks for carcinogenic PAHs

The estimation of relative toxicity of carcinogenic PAHs was performed by the toxicity equivalency factor (TEF) (US EPA, 2005). Thus, evaluating the toxicity and risks for environmental mixtures of carcinogenic PAHs in the examined sediments of China coastal zones was performed through TEFs as suggested by the US EPA (EPA, 1993). TEFs of DahA and BaP are 1, TEFs of BaA, InP and BbF are 0.1, TEF of BkF is 0.01, and TEF of Chr is 0.001 (US EPA, 1993). Toxic equivalents (TEQ) are sum of these seven PAHs, which is referred to BaP. TEQ at each site were calculated as follow:

$$TEQ = \sum_{i=1}^{n} Ci * TEFi$$

where C_i and TEF_i are the concentration and the TEF of individual congener, respectively.

2.7. Statistical analysis

All statistical analyses were performed using SPSS for windows (version 19.0, SPSS Inc., Chicago, IL, USA). The principal component analysis (PCA) with multiple linear regression analysis (MLR) was used to determine the sources of PAHs. Pearson's correlation analysis was performed to reveal the correlations among the PAHs, TOC and BC. All differences were tested for significance at $p = 0.05$.

3. Results

3.1. Concentration of BC_{Cr} and BC_{CTO}

The contents of BC_{Cr} and BC_{CTO} in the intertidal sediments are shown in the Table 1. High spatiotemporal variations in the concentrations of BC_{Cr} and BC_{CTO} were observed in the study area. Concentrations of BC_{Cr} in sediments varied between 0.61 and $6.32 \, mg \, g^{-1}$ in winter and between 1.20 and $5.93 \, mg \, g^{-1}$ in summer. The mean content of BC_{Cr} in the study area was slight lower in winter ($2.58 \pm 0.49 \, mg \, g^{-1}$) than in summer ($2.75 \pm 0.47 \, mg \, g^{-1}$). The contents of BC_{CTO} ranged from 0.66 to $3.39 \, mg \, g^{-1}$ and 0.57 to $4.76 \, mg \, g^{-1}$ in winter and summer, respectively (Table 1). The mean content of BC_{CTO} was significantly lower in winter ($1.73 \pm 0.24 \, mg \, g^{-1}$) than in summer ($2.14 \pm$

Table 1

Concentrations of TOC, BC and TN after chemical and thermal oxidation in intertidal sediments of China coastal zones.

Sites	TOC (mg g^{-1})	BC$_{Cr}$ (mg g^{-1})	BC$_{Cr}$/ TOC	BC$_{CTO}$ (mg g^{-1})	BC$_{CTO}$/ TOC	TN$_{Cr}$ (mg g^{-1})	TN$_{CTO}$ (mg g^{-1})
DD	8.69/4.48	0.61/2.02	0.07/0.45	0.66/1.38	0.08/0.31	0.39/0.21	0.21/0.30
TS	6.64/3.49	1.20/1.88	0.18/0.54	0.67/1.10	0.10/0.32	0.20/0.16	0.23/0.16
WF	17.63/14.24	1.50/2.07	0.09/0.14	2.05/0.57	0.12/0.04	0.23/0.12	0.25/0.17
QD	8.27/4.49	2.50/1.66	0.30/0.37	1.07/0.82	0.13/0.18	0.25/0.43	0.21/0.18
LYG	15.35/7.95	2.07/1.20	0.13/0.15	2.10/1.17	0.14/0.15	0.80/0.15	0.29/0.16
SH	7.77/3.78	3.46/1.17	0.45/0.31	1.38/1.53	0.18/0.40	0.47/0.41	0.37/0.35
WZ	5.98/8.62	2.27/2.32	0.38/0.27	2.59/1.94	0.43/0.23	0.39/0.44	0.38/0.30
FZ	9.82/6.12	2.59/3.49	0.26/0.57	1.10/2.45	0.11/0.40	0.26/0.16	0.30/0.27
XM	8.93/14.24	4.30/2.23	0.48/0.16	2.05/1.77	0.23/0.12	0.35/0.33	0.37/0.36
ST	5.90/7.61	2.05/4.14	0.35/0.54	3.39/2.04	0.57/0.27	0.43/0.04	0.40/0.09
ZH	12.87/8.95	2.13/4.92	0.17/0.55	2.46/4.17	0.19/0.47	0.56/0.58	0.38/0.63
BH	17.29/12.54	6.32/5.93	0.37/0.47	1.21/4.76	0.07/0.38	0.94/0.85	0.13/0.10

The numbers before the "/" represent the data for winter sediments, and the numbers after the "/" represent the data for summer sediments. The values are mean of triplicate analyses.

0.37 mg g^{-1}) ($p < 0.05$). Overall, low concentrations of both BC$_{Cr}$ and BC$_{CTO}$ were recorded at the sites DD to LYG, while higher concentrations were observed at the sites SH to BH (Table 1). It is noted that the mean concentration of BC$_{Cr}$ (2.67 ± 0.30 mg g^{-1}) was significantly higher than that of BC$_{CTO}$ (1.93 ± 0.22 mg g^{-1}) in the intertidal sediments of China coastal zones ($p < 0.05$).

3.2. Concentration and composition of PAHs

The contents of PAHs in the intertidal sediments are shown in the Fig. 2. High spatiotemporal variations in the concentrations of PAHs were observed in the study area. Specifically, concentrations of PAHs in the intertidal sediments ranged from 195.9 to 4610.2 ng g^{-1} in winter and 98.2 to 2796.5 ng g^{-1} in summer (Fig. 1). The mean content of PAHs in the study area was significantly higher in winter (2220.6 ± 459.9 ng g^{-1}) than in summer (607.9 ± 214.8 ng g^{-1}) ($p < 0.05$) (Fig. 3). In addition, PAH contents showed a distinctive latitudinal differentiation, with an increasing trend from high to low latitudes along the coastal zones of China (Fig. 3).

Compositions of PAH compounds differed in space and time (Fig. 4 and Table S1). In this study, PAHs in sediments collected in winter were dominated by four-ring PAH compounds (except for DD and BH), occupying 40.6–51.6% of total PAHs. However, five-ring plus six-ring PAH compounds accounted 8.1–24.0% of total PAHs (Fig. 4). The two-ring plus three-ring compounds, as the low PAH compound, contributed important fractions to total PAHs, especially in sites DD and BH, accounting for 26.9–72.2%. In summer, two-ring plus three-ring, four-ring and five-ring plus six-ring compounds occupied 6.9–75.2%, 8.4–65.1% and 10.6–56.9% of total PAHs, respectively. In addition, the high molecular weight PAHs (sum of fo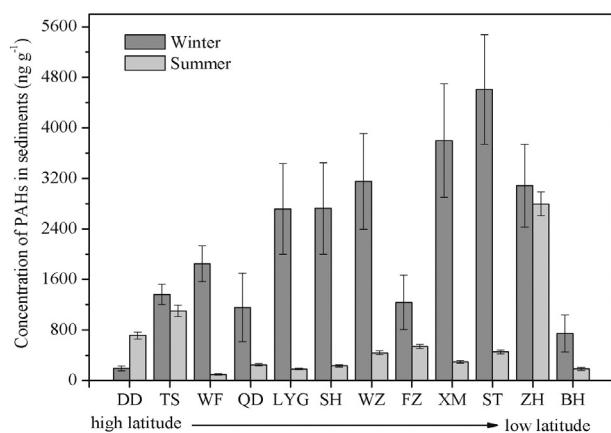ur, five and six-ring and five-ring compounds) were dominated at the sites from SH to BH (except for site BH), occupying 59.6–92.9% of total PAHs.

3.3. Links between BC and PAHs

The correlations of PAH compounds and TOC and BC are shown in Table 2. Sediment TOC was strongly related to Nap ($r = 0.72$, $p < 0.001$) and Phe ($r = 0.60$, $p = 0.002$). All Fl, Py, BaA, and Chry of four-ring compounds were significantly correlated with sediment TOC ($r = 0.58–0.61$, $p < 0.008$). In addition, sediment TOC were significantly related to total PAHs ($r = 0.61$, $p = 0.001$), low molecular weight (LMW) ($r = 0.62$, $p < 0.001$) and high molecular weight (HMW) compounds ($r = 0.59$, $p = 0.004$). However, no significant relationship of sediment TOC with BkF, InP, DahA derived from pyrolytic origin was observed ($p > 0.05$).

Sediment BC$_{Cr}$ was significantly related to some LWM compounds including Nap ($r = 0.43$, $p = 0.035$), Ace ($r = 0.44$, $p = 0.033$), Fluo ($r = 0.45$, $p = 0.026$). No significant correlation between BC$_{Cr}$ and PAHs, and LMW and HMW was observed ($r < 0.33$, $p > 0.05$). However, sediment BC$_{Cr}$ was not correlated closely with total PAHs, 3–6 ring compounds, LMW and HMW ($p > 0.05$). Sediment BC$_{CTO}$ was significantly related to all individual compounds (except for Nap, Phe, DahA and BghiP) ($p < 0.05$). Additionally, sediment BC$_{CTO}$ was strongly correlated with total PAHs, 3–6 ring compounds, LMW and HMW ($p < 0.05$). Overall, weaker relationship of sediment BC$_{Cr}$ with PAH compounds than relationship of sediment BC$_{CTO}$ with PAH compounds implied the PAHs derived from pyrolytic origin.

Fig. 2. Concentrations of PAHs in the intertidal sediments of China coastal zones. The bars are standard errors of triplicate.
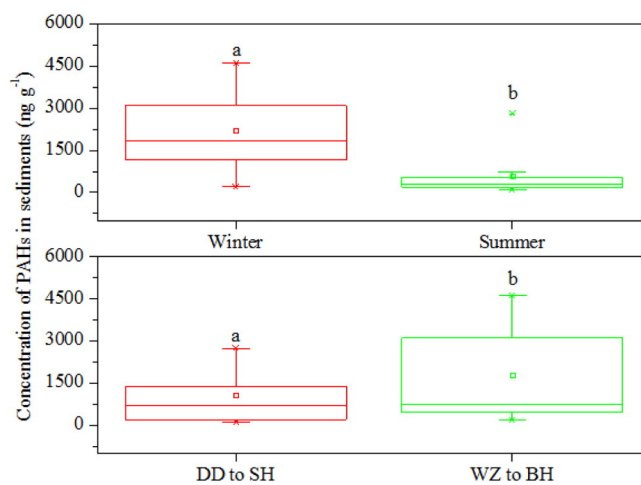

Fig. 3. Seasonal and spatial difference in concentration of PAHs in intertidal sediments of China coastal zones. The squares represent means and solid lines represent median values. Boxes enclose the interquartile range, whiskers show the full range. The letters indicated the statistically significant difference in means of PAH contents ($P < 0.05$).
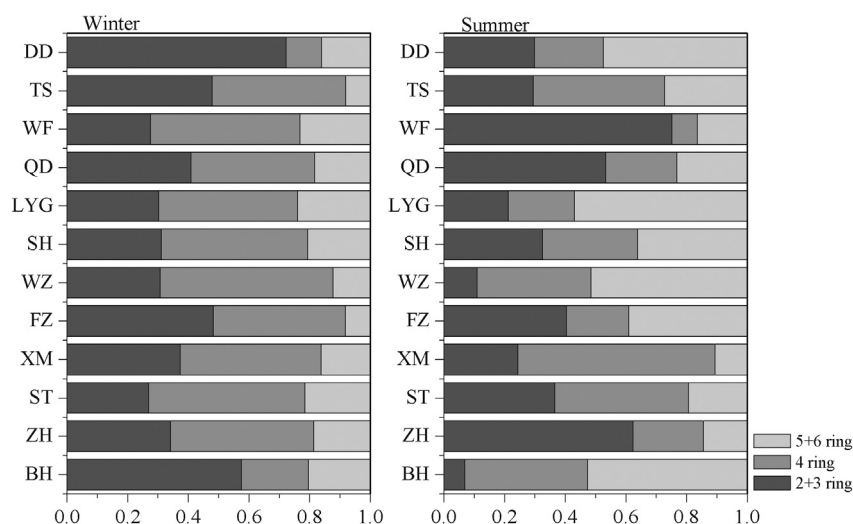
Fig. 4. Compositional profiles of PAH compounds in intertidal sediments taken in winter and summer.

3.4. $\delta^{13}C$ values of TOC and BC

The values of $\delta^{13}C$ in TOC were highly variable in space and time (Fig. 5). In this study, the values of $\delta^{13}C$ in TOC of intertidal sediments of China coastal zones ranged from $-21.13‰$ to $-24.87‰$ in winter and $-21.15‰$ to $-24.71‰$ in summer. However, average value of $\delta^{13}C$ was slight lower in winter ($-23.05 \pm 0.37‰$) than in summer ($-22.93 \pm 0.39‰$) (Fig. 5). In addition, the values of $\delta^{13}C$ in BC (BC_{CTO}) were highly variable in space but not time (Fig. 5). Mean value of the $\delta^{13}C$ in BC was $-21.59 \pm 0.71‰$ (ranging from $-23.53‰$ to $-16.78‰$) in winter and $-21.29 \pm 0.71‰$ (ranging from $-24.57‰$ to $-16.01‰$) in summer. It is worth noting that the most ^{13}C-depleted values in BC occurred in sites LYG, ZH and BH, while ^{13}C-enriched values in BC were observed at sites TS, WZ and XM (Fig. 5).

4. Discussion

4.1. BC and PAHs of different aquatic ecosystems

BC emission derives from combustion processes of fossil fuels and biomass, and is finally transported into sediments through river runoff and atmospheric deposition (Agarwal and Bucheli, 2011; Liu et al., 2012a). It has been reported that contents of BC in the harbor, estuarine, coastal, transportation, and Shelf sediments are significantly variable among transportations (Lohmann et al., 2005; Oen et al., 2006; Sánchez-García et al., 2010), especially between river runoff and atmospheric deposition (Wang et al., 2014b). In this study, high contents of BC were recorded at sites WZ, WZ, XM, ST, ZH and BH where are located in estuary and/or mangrove that likely receive large amount of BC

Table 2
Pearson's correlations of individual PAH compound and total PAHs to TOC and BC. The r represents correlation coefficient and *P* indicates significance level.

	Correlations to TOC		Correlations to BC_{Cr}		Correlations to BC_{CTO}	
	r	*P*	r	*P*	r	*P*
Nap	0.72	<0.001	0.43	0.035	0.29	0.17
Acy	0.40	0.054	−0.01	0.956	0.52	0.01
Ace	−0.004	0.986	0.44	0.033	0.56	0.004
Fluo	0.186	0.384	0.45	0.026	0.59	0.002
Phe	0.599	0.002	0.15	0.495	0.26	0.227
An	−0.06	0.777	0.09	0.681	0.63	0.001
Fl	0.61	0.002	0.20	0.361	0.42	0.041
Py	0.60	0.002	0.35	0.095	0.59	0.003
BaA	0.58	0.003	0.38	0.071	0.60	0.002
Chry	0.53	0.008	0.38	0.066	0.62	<0.001
BbF	0.60	0.002	0.32	0.132	0.53	0.008
BkF	0.19	0.378	0.42	0.039	0.73	<0.001
BaP	0.41	0.046	0.22	0.306	0.56	0.005
InP	−0.05	0.818	0.17	0.435	0.46	0.023
DahA	0.24	0.251	0.41	0.047	0.33	0.112
BghiP	0.52	0.009	0.18	0.404	0.31	0.139
2-ring	0.72	<0.001	0.43	0.035	0.29	0.17
3-ring	0.50	0.012	0.24	0.266	0.55	0.006
4-ring	0.62	0.001	0.30	0.152	0.54	0.006
5-ring	0.51	0.012	0.38	0.069	0.68	<0.001
6-ring	0.24	0.26	0.25	0.240	0.50	0.013
LMW	0.62	<0.001	0.32	0.145	0.53	0.007
HMW	0.59	0.004	0.33	0.125	0.60	0.002
PAHs	0.61	0.001	0.33	0.112	0.59	0.002

2-ring include Nap; 3-ring include Acy, Ace, Fluo, Phe, An; 4-ring include Fl, Py, BaA, Chry; 5-ring include BbF, BkF, BaP; 6-ring include InP, DahA, BghiP. LMW was abbreviations for low molecular weight, and HMW was abbreviations for high molecular weight.
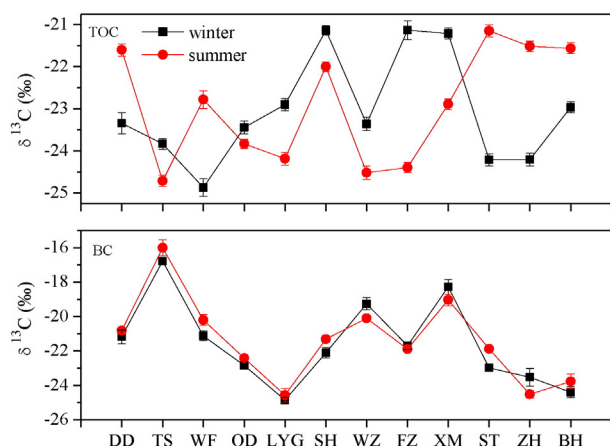
Fig. 5. Spatial–temporal variations of $\delta^{13}C$ in total organic carbon and black carbon of the intertidal sediments of China coastal zones.

through river runoff. However, relatively low contents of BC in the coastal sediments of sites QD, WF and LYG were observed. Therefore, these results suggest that river flows can be attributed as a more serious pathway to BC contamination in sediments compared to atmospheric deposition.

The mean concentration of BC_{CTO} (1.81 ± 0.29 mg g^{-1}) in this study was comparable to those in sediments of Swedish continental shelf (2.41 ± 0.46 mg g^{-1}) (Sánchez-García et al., 2010), lower than those in harbor sediments of Norwegian (3.39 ± 1.9 mg g^{-1}) (Oen et al., 2006) and harbor sediments of Boston and New York (4.70 ± 0.53 mg g^{-1}) (Lohmann et al., 2005), but higher than in estuarine and coastal sediment (0.40 ± 0.30–1.20 ± 0.18 mg g^{-1}) (Table 3). The comparison results suggest that the harbor sediments were heavily polluted by BC that derives from the combustion of diesel fuels. In this study, the mean values of BC_{Cr}/TOC and BC_{CTO}/TOC ratios were 0.37 ± 0.03 and 0.27 ± 0.03, respectively. The value of BC_{CTO}/TOC ratio in the present study was comparable to that of estuary sediments of Taiwan (Hung et al., 2010), but higher than that of other sediments (Table 3). The low ratios reported in previous studies may be attributed to high contents of TOC in shelf, estuary and harbor sediments (Table 3).

The concentration of PAHs in the study ranged from 98.2 ng g^{-1} to 4610.2 ng g^{-1}, with a mean value of 1414.3 ± 334.5 ng g^{-1}. Generally, high contents of PAHs were observed at the sites SH, WZ, XM, ST and ZH (Fig. 2). The reason was likely attributed to that these sites are located in estuary and/or mangrove that can receive substantial amount of pollutants through river flows and groundwater runoff (Mai et al., 2003). The mean concentrations of PAHs in this study were higher than those in Minjiang estuary (669.2 ng g^{-1}, Yuan et al., 2001), Bohai (481 ng g^{-1}, Li et al., 2015), Zhanjiang Bay (351.98 ng g^{-1}, Huang et al., 2012) and in the Pearl River estuary (563.78 ng g^{-1}, Zhang et al., 2015). However, the contents of PAHs reported in Norwegian harbor sediments (Oen et al., 2006), Naples harbor (Sprovieri et al., 2007) and Bhavnagar harbor (Dudhagara et al., 2016) were significantly higher than those in this

study (Table 4). Because these sites are the harbors which is likely suffered from diesel combustion from a large amount of ships.

It has been reported that North coastal zones of China are heavily affected by coke industry and fossil energy consumption, which result in high PAH pollution in these zones (Liu et al., 2012b). In this study, however, the mean content of PAHs was significantly lower at sites DD to SH than at sites WZ to BH ($p < 0.05$) (Fig. 3). In addition, the PAHs were highly variable in space and increased dramatically from North to South sampling sites (except for ZH). The sampling sites in previous study (Liu et al., 2012a, 2012b) were in the continental shelf zones of China sea and the accumulations of PAHs in these sites were thus mainly depended on the atmospheric deposition resulting from mainland emissions. In the present study, most sampling sites were situated in estuaries/mangrove where can receive PAHs largely from river flows and groundwater runoff. Therefore, the contents of PAHs were significantly lower in continental shelf sediments (19–203 ng g^{-1}, Liu et al., 2012b) than coastal sediments of China (98.2–4610.2 ng g^{-1}, Fig. 2). These results indicated that estuarine and coastal sediments are seriously contaminated by PAHs, especially in extensive anthropogenic activities area. However, the BC-derived PAH deposition and its associated sedimentary process have great influence on the distribution and behavior of PAHs in the estuarine and coastal environments (Meijer et al., 2008; Lin et al., 2013; Lin et al., 2013; Moeckel et al., 2013). In addition, the differences of regional fossil energy consumption of China could partly result in the spatiotemporal variations in PAH pollution of the intertidal sediments along China coastal zones (Guo et al., 2006; Liu et al., 2012a, 2012b; Lin et al., 2013).

4.2. Evaluation of toxicity and risks for carcinogenic PAHs

Seven potentially carcinogenic PAHs including BaA, Chr, BbF, BkF, BaP, DahA and InP were used to evaluate the toxicity (Sarria-Villa et al., 2016). The amounts of these seven PAHs ranged from 35.6 ng g^{-1} (DD) to 1427.4 ng g^{-1} (ST) with a mean value of 583.6 ng g^{-1} in winter, while varied between 22.4 ng g^{-1} (WF) and 1215.4 ng g^{-1} (ZH) with an average value of 231.8 ng g^{-1} in summer. These values (except for site ST in winter) were lower than the effect range low (ERL) value of 1373 ng g^{-1} (Long et al., 1995). In addition, total TEQ in the study area ranged from 19.9 to 294.9 ng BaP g^{-1} in winter and from 6.2 to 169.9 ng BaP g^{-1} in summer (Fig. S1). The mean value of TEQ was significantly higher in winter (110.1 ng BaP g^{-1}) than in summer (44.6 ng BaP g^{-1}) ($p < 0.05$). The high values of TEQ were recorded at sites ST, LYG, XM and ZH for winter, while ZH, DD and TS for summer (Fig. S1). The values of TEQ in the study area were higher than that in Bohai Sea (5.95–68.8 ng BaP g^{-1}, Li et al., 2015), while lower than that in Barents Sea (18–300 ng BaP g^{-1}, Savinov et al., 2003), Naples harbor (2–4723 ng BaP g^{-1}, Sprovieri et al., 2007), Kaosiung harbor (3.9–1970 ng BaP g^{-1}, Chen et al., 2013), Meiliang Bay (94–856 ng BaP g^{-1}, Qiao et al., 2006) and comparable to Barents Sea (18–300 ng BaP g^{-1}, Savinov et al., 2003) (Table S2). Overall, these comparison results imply low potential carcinogenicity of PAHs and may not pose ecological risk to the intertidal sediments of China coastal zones.

Table 3
Comparison of BC, TOC and BC/TOC in sediments from different parts of the world.

Sample types	Method	BC (mg g^{-1})	TOC (mg g^{-1})	BC/TOC	References
Coastal sediment	Cr$_2$O$_7$	2.96 ± 0.47	8.99 ± 1.01	0.37 ± 0.03	This study
	CTO375	1.81 ± 0.29		0.27 ± 0.03	
Shelf sediment	CTO375	1.20 ± 0.18	29.9 ± 2.80	0.04	Gustafsson and Gschwend (1998)
Estuary sediment	CTO375	0.40 ± 0.30	8.80 ± 2.60	0.05 ± 0.03	Sánchez-García et al. (2013)
Shelf sediment	CTO375	2.41 ± 0.46	46.7 ± 15.3	0.06 ± 0.02	Sánchez-García et al. (2010)
Harbor sediment	CTO375	3.39 ± 1.90	38.25 ± 13.14	0.07 ± 0.02	Oen et al. (2006)
Estuary sediment	CTO375	0.60 ± 0.06	4.11 ± 0.90	0.22 ± 0.03	Hung et al. (2010)
Coastal sediment	CTO375	0.95 ± 0.12	7.65 ± 1.27	0.14 ± 0.01	Hung et al. (2007)
Harbor sediment	CTO375	4.70 ± 0.53	28.5 ± 1.02	0.16 ± 0.01	Lohmann et al. (2005)

Table 4
Concentrations of PAHs in the sediments from different parts of the world.

Country	Sites	PAHs	Range (ng g^{-1})	Mean (ng g^{-1})	References
China	Bohai	16	149–1211	481	Li et al., 2015
China	Zhanjiang Bay	16	41.96–933.9	315.98	Huang et al. 2012
China	Pearl river estuary	16	119.49–3828.58	563.78	Zhang et al., 2015
China	Minjiang estuary	16	316.0–1260.0	669.2	Yuan et al., 2001
India	Bhavnagar harbor	16	5020–981,180	345,000	Dudhagara et al., 2016
Norwegian	Norwegian harbor	16	2000–76,000	–	Oen et al., 2006
Guba	Pechenga	16	428–3257	–	Savinov et al., 2003
Swedish	continental shelf	15	120–9600	–	Sánchez-García et al., 2010
Italy	Naples harbor	16	9–31,774	–	Sprovieri et al., 2007

4.3. Effects of TOC and BC$_{CTO}$ on PAHs

Previous studies have reported that PAHs are usually related with TOC due to low solubility and hydrophobic nature of PAHs (Countway et al., 2003; Hung et al., 2007; Lin et al., 2013). In this study, sediment TOC was strongly related to the Nap and Phe derived from petrogenic sources ($p < 0.05$) (Table 2). All Fl, Py, BaA, and Chry of four-ring compounds were significantly correlated with sediment TOC. In addition, sediment TOC were significantly related to total PAHs, low molecular weight (LMW) and high molecular weight (HMW) compounds ($p < 0.05$). However, no significant relationship of sediment TOC with BkF, InP, DahA derived from pyrolytic origin was observed ($p > 0.05$). Sediment BC$_{CTO}$ was significantly related to all individual compounds (except for Nap, Phe, DahA and BghiP) ($p < 0.05$). Additionally, sediment BC$_{CTO}$ was strongly correlated with total PAHs, 3–6 ring compounds, LMW and HMW ($p < 0.05$). In addition, TOC generally showed weaker correlations than BC$_{CTO}$ with HMW PAH compounds, indicating that PAH sorption in the sediments was BC-dominated (Wiedemeier et al., 2015).

The results presented in Table 2 on the correlations of individual and total examined PAHs with both TOC and BC highlight the fact that 2- and 4-ring compounds are primarily related to TOC rather than BC, while in fact 3- and 5-ring compounds are also significantly correlated to TOC (Oen et al., 2006; Sánchez-García et al., 2010). Five compounds (Acy, Ace, Fluo, An, BkF, InP) correlated primarily to BC and another six compounds (FI, Py, BaA, Chry, BBF, and BaP) strongly correlated to both TOC and BC (Table 2). Therefore, these results indicated that the compounds of PAHs from pyrolytic origins were mainly regulated by BC in the sedimentary environments (Lohmann et al., 2005; Oen et al., 2006; Sánchez-García et al., 2010). This conclusion is supported by the findings that sorption capacities of BC with the large pore surfaces have potential influence on the pyrogenic PAH distributions (Oen et al., 2006). In this study, the good correlations observed for the examined 2- and 4-ring compounds, and secondarily 3-ring compounds to TOC probably indicate the accumulation of BC on organic rich detritus and/or significant fossil inputs in the study area (Accardi-Dey and Gschwend, 2002, 2003). Therefore, theses correlation results indicate likely that the distribution of the PAH compounds is driven by the partitioning between natural organic carbon and combustion-derived black carbon (Accardi-Dey and Gschwend, 2002, 2003).

It is reported that BC likely constitute a part of TOC due to that BC has recalcitrant character and is resistant to degradation (Sánchez-García et al., 2012). In this study, the TOC contents were in the range of 3.49–17.63 mg g^{-1} of the sediment dry weight (Table 1). The contents of BC in the sediments ranged from 0.57 to 4.76 mg g^{-1}, which contributed 4–57% of TOC (Table 1). The BC fractions were lowest in the sites WF and LYG (4–15% of TOC) and highest in the sites WZ, SH, and ST (18–57% of TOC). The BC determined with the same CTO-375 method accounted for 14% of TOC in the Taiwan coastal sediments (Hung et al. (2007). Therefore, the high values of BC$_{CTO}$/TOC were observed due to high contents of BC in the intertidal sediments of China coastal zones. Generally, the contents of BC$_{CTO}$ were higher in harbor sediments than in other

aquatic sediments (Table 3), indicating that oil fuel combustion contributed mostly to BC of aquatic ecosystems. The BC$_{CTO}$/TOC ratio was higher in the harbor sediments of Boston and New York (Lohmann et al., 2005), while the unexpected low BC$_{CTO}$/TOC ratios in the Norwegian harbor sediments may be likely attributed to the high concentrations of TOC (Oen et al., 2006) (Table 3). However, there may be an overestimation of BC$_{CTO}$/TOC ratios due to that the analytical methods of BC may potentially lead to higher contents of measured BC compared to in situ sediments.

4.4. TOC, BC and PAH source identification

4.4.1. TOC and BC identified by the values of $\delta^{13}C$

The $\delta^{13}C$ values of TOC ranged from $-18.23‰$ to $-25.69‰$ with a mean of $-22.86‰$ in Bohai sediments (Gao et al., 2012). In contrast, a relative small variations of $\delta^{13}C$ values of TOC were observed in East China Sea sediments, ranging from $-20.1‰$ to $-22.7‰$ (Xing et al., 2011). In this study, the $\delta^{13}C$ values of TOC in our samples ranged from $-21.13‰$ to $-24.87‰$ with significant seasonal differences (Fig. 5), and were similar to the TOC decreasing trend. It is reported that the end-member $\delta^{13}C$ values are $-25.6‰$ for Changjiang River organic matter and $-20‰$ for marine organic matter (Xing et al., 2011). In addition, the $\delta^{13}C$ values of marine derived organic matter ranged from $-18‰$ to $-22‰$) (Ramaswamy et al., 2008), while the values of fluvial organic carbon varied from $-24‰$ to $-28‰$ (Lamb et al., 2006). In this study, the $\delta^{13}C$ values in the intertidal sediments varied between $-21.13‰$ and $-24.87‰$. Therefore, the $\delta^{13}C$ values of TOC in this study indicate a mixed marine/terrestrial origin for organic matter in the intertidal sediments of China coastal zones. It was worth noting that $\delta^{13}C$ values in TOC in the study area were highly variable, the reason may be attributed to the decomposition processes of organic matter and the differences of environmental conditions (Gao et al., 2012; Wu et al., 2013).

The values of the $\delta^{13}C$ in BC of intertidal sediments ranged from $-23.53‰$ to $-16.78‰$ for winter and from $-24.57‰$ to $-16.01‰$ for summer (Fig. 5). The significant difference in $\delta^{13}C$ of BC in these sediment samples clearly indicate the BC come form different residues of fossil fuels and biomass. The lowest values of $\delta^{13}C$ in BC were observed at sites QD, LYG, ST, ZH and BH, likely indicate that fossil fuel contributes mostly to the BC in the sediment due to that combustion of fossil fuel can lead to ^{13}C depletion (Petrisic et al., 2013). It is also reported that the $\delta^{13}C$ values in BC decreased with the increasing contents of BC in soils (Hamilton and Hartnett, 2013). Very high $\delta^{13}C$ value of BC in site TS may suggest the BC derived mainly from natural origins (Hamilton and Hartnett, 2013). The BC mainly derived from incomplete combustion of fossil fuels and biomass (Koelmans et al., 2006; Agarwal and Bucheli, 2011) and has stability that delays its degradation, thus it has been considered to reveal not only the sources of PAHs (Accardi-Dey and Gschwend, 2002; Lohmann et al., 2005), but also identify the sources of anthropogenic carbon in sediments (Agarwal and Bucheli, 2011; Sánchez-García et al., 2012). It is worth noting that no seasonal change in those $\delta^{13}C$ values in BC was observed, likely due to their

stability which delays their degradation (Accardi-Dey and Gschwend, 2002; Lohmann et al., 2005). Furthermore, there was a distinctly spatial heterogeneity of $\delta^{13}C$ values of BC among these sampling sites. These results indicated stable and different sources of BC in the intertidal sediments of China coast zones.

However, source apportionment of BC based on $\delta^{13}C$ values is difficult. The $\delta^{13}C$ values of coal combustion were observed to correspond to more ^{13}C-depletion with increased temperature of formation (Petrisic et al., 2013). In addition, carsoot and wood burning contribute different ^{13}C depletion, due to that the combustion temperatures result in the different BC characteristic (Oen et al., 2006; Sánchez-García et al., 2010). Although the $\delta^{13}C$ values of BC in our study could be associated closely with the different fuels combustion (fossil fuels and biomass), the actual $\delta^{13}C$ values in the intertidal sediments are quite different. The spatial variations in $\delta^{13}C$ values of BC was observed among the sediment samples and could indicate that other processes such as weathering, microbial degradation and tidal events erosion may have influenced the isotopic composition (Liu et al., 2013; Petrisic et al., 2013). Therefore, further research should consider the discussion on carbon isotopic signatures of individual PAHs and benzene polycarboxylic acids (BPCA) analysis (even $\delta^{13}C$ of individual BPCA), which provides a more valuable tool to delineate PAH sources in aquatic sediments (Wiedemeier et al., 2015).

4.4.2. PAH sources determined by MDR and PCA-MLR

Molecular diagnostic ratios (MDR) of PAHs are widely used to diagnose sources because different diagnostic ratios indicate special source (Yunker et al., 1996; Yunker et al., 2002; Lin et al., 2011). In this study, the BaA/(BaA + CHR) ratios at all sites (except for DD collected in winter) were >0.35 and all FLUO/(FLUO + PYR) ratios (except site ZH collected in summer) were above 0.5 (Fig. 6a), which indicated that the biomass and coal combustion were the pyrogenic sources of PAHs (Yunker et al., 2002). In terms of the ratios of ∑LMW/∑HMW, the values

suggested that the PAHs derived from pyrogenic sources at almost sites (Barakat et al., 2011) (Fig. 6b). The AN/(AN + PHE) ratios at most sampling sites being more than 0.1 indicated pyrogenic sources, while the ratios at some sites being less than 0.1 suggested that the parent compounds of PAHs is of fossil origin (Fig. 6c) (Yunker et al., 2002). The InP/(InP + BghiP) ratios at most sampling sites indicated pyrogenic sources of grass, wood or coal combustion, ratios at other sites pointed to mixed sources such as petroleum and liquid fossil fuel. The InP/(InP + BghiP) ratios of sampling sites indicated seasonal variations of PAH sources in the intertidal sediments of China coastal zones (Fig. 6d). Because most PAHs in estuary environments result from river runoff, it seems likely that the sources of the studied PAH compounds are similar to those of rivers. Previous studies reported that the combustions of grass, wood and coal could be possible sources of PAHs in the Yellow River (Li et al., 2006) and the PAHs of sediments in Yangtze River derived from coal and wood burning (Feng et al., 2007). PAHs of sediments in Minjiang River derived mainly from incomplete combustion of fossil fuels (Zhang et al., 2004). In addition, crude oil and sewage discharges were likely the sources of PAHs in Jiulong River (Maskaoui et al., 2002) and a mixed energy structure such as wood, coal and petroleum combustion of pyrolytic inputs were the sources of PAHs in the Pearl River (Zhang et al., 2015). Overall, these results indicated that the PAHs derived mainly from the pyrogenic sources of biomass and fossil fuels combustions in estuarine and coastal sediments.

However, principal component analysis (PCA) with multiple linear regression analysis (MLR) has been well used to determine the quantitative contributions to the identified PAH sources (Sofowote et al., 2008). Previous studies have suggested that BkF was identified as a marker of diesel emissions, BghiP plus BaP and InP were found to derive from a mix of oil and coal emissions (Larsen and Baker, 2003). In addition, Py, BaA and Chry as the indicators of coal combustion have been reported by Simcik et al. (1999). In this study, component matrix identified by principal component analyses indicated that the first
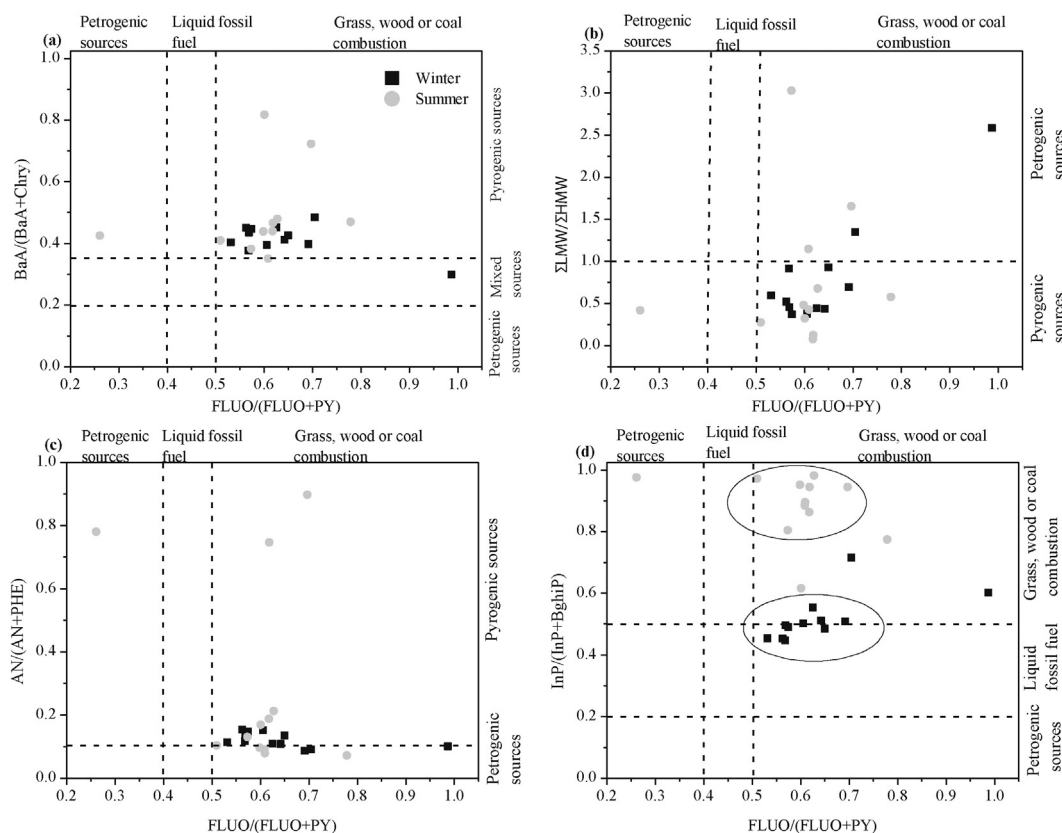

Fig. 6. Bivariate plots of molecular diagnostic ratios for samples; (a) BaA /(BaA + Chry) vs. FLUO/(FLUO + PY); (b) ∑LMW/∑HMW vs. FLUO/(FLUO + PY); (c); AN/(AN + PHE) vs. FLUO/(FLUO + PYR) and (d) InP/(InP + BghiP) vs. FLUO/(FLUO + PY).

Table 5
Rotated component matrix of individual compound PAH in intertidal sediments of China coastal zones.

PAHs	Winter			Summer			
	F_1	F_2	F_3	F_1	F_2	F_3	F_4
Nap	**0.856**	−0.226	0.155	0.510	−0.296	−0.204	**0.524**
Acy	0.189	−0.071	**0.959**	−0.088	−0.213	−0.208	**0.813**
Ace	−0.274	0.559	**0.685**	**0.919**	−0.04	0.200	0.294
Fluo	0.161	**0.957**	−0.021	**0.908**	−0.005	0.172	0.326
Phe	0.489	**0.790**	0.035	**0.629**	0.082	0.736	−0.109
An	0.619	**0.675**	0.115	0.195	0.035	**0.966**	−0.015
Fl	0.607	**0.731**	0.102	0.468	0.486	**0.666**	−0.183
Py	**0.674**	0.663	0.221	**0.936**	0.140	0.291	−0.109
BaA	**0.930**	0.317	−0.023	**0.960**	0.077	0.182	−0.140
Chry	**0.918**	0.334	−0.069	**0.964**	0.040	0.206	−0.102
BbF	**0.919**	0.350	−0.039	**0.959**	0.073	0.201	−0.126
BkF	**0.852**	0.393	−0.141	**0.892**	−0.031	0.092	−0.087
BaP	**0.829**	0.325	0.328	**0.663**	0.662	0.270	−0.128
InP	**0.840**	0.428	0.004	0.067	**0.892**	0.153	−0.079
DahA	**0.677**	0.523	0.141	−0.082	0.184	0.113	**0.944**
BghiP	**0.843**	0.430	0.079	−0.127	**0.971**	−0.057	0.041
Variance/%	68.24	12.68	8.93	53.72	18.59	11.84	7.60
Cumulative/%	68.24	80.92	89.85	53.72	72.31	84.15	91.75

Factor loadings are higher in the factor shown in bold.

component has high correlations with 4-, 5- and 6-ring in winter and 3- and 5-ring PAHs in summer, respectively (Table 5). Thus, the first component for winter was assigned to oil and coal combustions sources, while coal combustion and vehicular emissions were identified (Glaser et al., 2005). The second component was highly loaded in Ace, Fluo, and Phe in winter and InP and BghiP in summer, indicating that these compounds derived from coal and liquid fossil fuel combustion, respectively. The third component suggested that oil combustion and oil spill were the main sources in winter and coal emissions were the possible source in summer. The relative contribution of 52.53% was attributed to the mixed sources of oil spill, biomass and oil combustion and vehicular emissions, 38.80% was identified as coal combustion, minor fraction of 8.67% was tentatively assumed source of oil combustion and oil spill in winter (Table S4). In summer, vehicular emissions and coal combustion contribute 56.38% to total sources, and 12.23% of total sources were attributed to oil combustion, while 31.32% to the coal combustion (Table S4). According to the results discussed above, the PAH sources of study area derived mainly from the pyrogenic residues of various fuels combustion, emphasizing the primary contribution of pyrogenic sources to the intertidal sediments of China coastal zones.

5. Conclusion

This study provides spatiotemporal differences of PAHs and BC and reveals the effects of TOC and BC on PAHs in the intertidal sediments of China coastal zones. TOC, BC and PAHs were highly variable in space and time, may due to the differences of energy structures and sedimentary environments. Greater PAH accumulations in the sediments of estuarine environments suggested that rivers runoff may have been responsible for the general higher PAH pollution levels in the intertidal sediments of China coastal zones. The results of potential toxicity assessment indicated low ecological risk in the intertidal sediments of China coastal zones. Pearson's correlation analysis suggested that TOC contents were strongly correlated with the petrogenic compounds of PAHs, because these compounds derived from natural sources. However, pyrogenic compounds of PAHs were significantly related to BC, due to that BC and these compounds derived mainly from the combustion process of fossil fuels and biomass. Overall, increasing energy consumptions caused by anthropogenic activities can contribute to more emissions of BC as well as PAHs and thus improve the importance of BC in indicating pyrogenic compounds of PAHs in the intertidal sediments of China coastal zones.

Appendix A. Supplementary data

Supplementary data to this article can be found online at http://dx.doi.org/10.1016/j.scitotenv.2016.05.212.

References

Accardi-Dey, A., Gschwend, P.M., 2002. Assessing the combined roles of natural organic matter and black carbon as sorbents in sediments. Environ. Sci. Technol. 36, 21–29.

Accardi-Dey, A., Gschwend, P.M., 2003. Reinterpreting literature sorption data considering both absorption into organic carbon and adsorption onto black carbon. Environ. Sci. Technol. 37, 99–106.

Agarwal, T., Bucheli, T.D., 2011. Is black carbon a better predictor of polycyclic aromatic hydrocarbon distribution in soils than total organic carbon. Environ. Pollut. 159, 64–70.

Barakat, A.O., Mostafa, A., Wade, T.L., Sweet, S.T., El Sayed, N.B., 2011. Distribution and characteristics of PAHs in sediments from the Mediterranean coastal environment of Egypt. Mar. Pollut. Bull. 62 (9), 1969–1978.

Chen, C.F., Chen, C.W., Dong, C.D., Kao, C.M., 2013. Assessment of toxicity of polycyclic aromatic hydrocarbons in sediments of Kaohsiung Harbor, Taiwan. Sci. Total Environ. 463, 1174–1181.

Countway, R.E., Dickhut, R.M., Canuel, E.A., 2003. Polycyclic aromatic hydrocarbon (PAH) distributions and associations with organic matter in surface waters of the York River, VA Estuary. Org. Geochem. 34, 209–224.

Dudhagara, D.R., Rajpara, R.K., Bhatt, J.K., Gosai, H.B., Sachaniya, B.K., Dave, B.P., 2016. Distribution, sources and ecological risk assessment of PAHs in historically contaminated surface sediments at Bhavnagar coast, Gujarat, India. Environ. Pollut. 213, 338–346.

Feng, C.L., Xia, X.H., Shen, Z.Y., Zhou, Z., 2007. Distribution and sources of polycyclic aromatic hydrocarbons in Wuhan section of the Yangtze River, China. Environ. Monit. Assess. 133 (1–3), 447–458.

Gao, X.L., Yang, Y.W., Wang, C.Y., 2012. Geochemistry of organic carbon and nitrogen in surface sediments of coastal Bohai Bay inferred from their ratios and stable isotopic signatures. Mar. Pollut. Bull. 64 (6), 1148–1155.

Glaser, B., Dreyer, A., Bock, M., Fiedler, S., Mehring, M., Heitmann, T., 2005. Source apportionment of organic pollutants of a highway-traffic-influenced urban area in Bayreuth (Germany) using biomarker and stable carbon isotope signatures. Environ. Sci. Technol. 39, 3911–3917.

Guo, Z.G., Lin, T., Zhang, G., Yang, Z.S., Fang, M., 2006. High-resolution depositional records of polycyclic aromatic hydrocarbons in the central continental shelf mud of the East China Sea. Environ. Sci. Technol. 40 (17), 5304–5311.

Gustafsson, Ö, Gschwend, P.M., 1998. The flux of black carbon to surface sediments on the New England continental shelf. Geochim. Cosmochim. Ac 62 (3), 465–472.

Gustafsson, O., Bucheli, T.D., Kukulska, Z., Andersson, M., Largeau, C., Rouzaud, J.N., Reddy, C.M., Eglinton, T.I., 2001. Evaluation of a protocol for the quantification of black carbon in sediments. Glob. Biogeochem. Cycles 15 (4), 881–890.

Hamilton, G.A., Hartnett, H.E., 2013. Soot black carbon concentration and isotopic composition in soils from an arid urban ecosystem. Org. Geochem. 59, 87–94.

Huang, W.X., Wang, Z.Y., Yan, W., 2012. Distribution and sources of polycyclic aromatic hydrocarbons (PAHs) in sediments from Zhanjiang Bay and Leizhou Bay, South China. Mar. Pollut. Bull 64, 1962–1969.

Hung, C.C., Gong, G.C., Chen, H.Y., Hsieh, H.L., Santschi, P.H., Wade, T.L., Sericano, J.L., 2007. Relationships between pesticides and organic carbon fractions in sediments of the Danshui River estuary and adjacent coastal areas of Taiwan. Environ. Pollut. 148 (2), 546–554.

Hung, C.C., Gong, G.C., Ko, F.C., Chen, H.Y., Hsu, M.L., Wu, J.M., Peng, S.C., Nan, F.H., Yeager, K.M., Santschi, P.H., 2010. Relationships between persistent organic pollutants and carbonaceous materials in aquatic sediments of Taiwan. Mar. Pollut. Bull. 60 (7), 1010–1017.

Inomata, Y., Kajino, M., Sato, K., Ohara, T., Kurokawa, J.I., Ueda, H., Tang, N., Hayakawa, K., Ohizumi, T., Akimoto, H., 2012. Emission and atmospheric transport of particulate PAHs in Northeast Asia. Environ. Sci. Technol. 46, 4941–4949.

Jautzy, J., Ahad, J.M.E., Gobeil, C., Savard, M.M., 2013. Century-long source apportionment of PAHs in Athabasca oil sands region lakes using diagnostic ratios and compound-specific carbon isotope signatures. Environ. Sci. Technol. 47, 6155–6163.

Koelmans, A.A., Jonker, M.T.O., Cornelissen, G., Bucheli, T.D., Van Noort, P.C.M., Gustafsson, O., 2006. Black carbon: the reverse of its dark side. Chemosphere 63, 365–377.

Laflamme, R.E., Hites, R.A., 1978. The global distribution of polycyclic aromatic hydrocarbons in recent sediments. Geochim. Cosmochim. Acta 42 (3), 289–303.

Lamb, A.L., Wilson, G.P., Leng, M.J., 2006. A review of coastal palaeoclimate and relative sea-level reconstructions using δ^{13}C and C/N ratios in organic material. Earth-Sci. Rev. 75, 29–57.

Lang, C., Tao, S., Liu, W.X., Zhang, Y.X., Simonich, S., 2008. Atmospheric transport and outflow of polycyclic aromatic hydrocarbons from China. Environ. Sci. Technol. 42, 5196–5201.

Larsen, R.K., Baker, J.E., 2003. Source apportionment of polycyclic aromatic hydrocarbons in the urban atmosphere: a comparison of three methods. Environ. Sci. Technol. 37, 1873–1881.

Li, G.C., Xia, X.H., Yang, Z.F., Wang, R., Voulvoulis, N., 2006. Distribution and sources of polycyclic aromatic hydrocarbons in the middle and lower reaches of the Yellow River, China. Environ. Pollut. 144 (3), 985–993.

Li, J.F., Dong, H., Zhang, D.H., Han, B., Zhu, C.J., Liu, S.P., Liu, X.M., Ma, Q.Y., Li, X.G., 2015. Sources and ecological risk assessment of PAHs in surface sediments from Bohai Sea and northern part of the Yellow Sea, China. Mar. Pollut. Bull. 96 (1), 485–490.

Lim, B., Cachier, H., 1996. Determination of black carbon by chemical oxidation and thermal treatment in recent marine and lake sediments and Cretaceous-Tertiary clays. Chem. Geol. 131, 143–154.

Lin, T., Hu, L.M., Guo, Z.G., Qin, Y.W., Yang, Z.S., Zhang, G., Zheng, M., 2011. Sources of polycyclic aromatic hydrocarbons to sediments of the Bohai and Yellow Seas in East Asia. J. Geophys. Res. Atmos. 116 (D23). http://dx.doi.org/10.1029/2011JD015722.

Lin, T., Hu, L.M., Guo, Z.G., Zhang, G., Yang, Z.S., 2013. Deposition fluxes and fate of polycyclic aromatic hydrocarbons in the Yangtze River estuarine-inner shelf in the East China Sea. Glob. Biogeochem. Cycles 27 (1), 77–87.

Liu, L.Y., Wang, J.Z., Wei, G.L., Guan, Y.F., Wong, C.S., Zeng, E.Y., 2012a. Sediment records of polycyclic aromatic hydrocarbons (PAHs) in the continental shelf of China: implications for evolving anthropogenic impacts. Environ. Sci. Technol. 46, 6497–6504.

Liu, L.Y., Wan, J.Z., We, G.L., Guan, Y.F., Zeng, E.Y., 2012b. Polycyclic aromatic hydrocarbons (PAHs) in continental shelf sediment of China: implications for anthropogenic influences on coastal marine environment. Environ. Pollut. 167, 155–162.

Liu, Y., Beckingham, B., Ruegner, H., Li, Z., Ma, L.M., Schwientek, M., Xie, H., Zhao, J.F., Grathwohl, P., 2013. Comparison of sedimentary PAHs in the rivers of Ammer (Germany) and Liangtan (China): differences between early- and newly-industrialized countries. Environ. Sci. Technol. 47, 701–709.

Lohmann, R., MacFarlane, J.K., Gschwend, P.M., 2005. Importance of black carbon to sorption of native PAHs, PCBs, and PCDDs in Boston and New York harbor sediments. Environ. Sci. Technol. 39 (1), 141–148.

Long, E.R., MacDonald, D.D., Smith, S.L., Calder, F.D., 1995. Incidence of adverse biological effects within ranges of chemical concentrations in marine and estuarine sediments. Environ. Manag. 19, 81–97.

Mai, B.X., Qi, S.H., Zeng, E.Y., Yang, Q.S., Zhang, G., Fu, J.M., Sheng, G.Y., Peng, P.A., Wang, Z.S., 2003. Distribution of polycyclic aromatic hydrocarbons in the coastal region off Macao, China: assessment of input sources and transport pathways using compositional analysis. Environ. Sci. Technol. 37, 4855–4863.

Maskaoui, K., Zhou, J.L., Hong, H.S., Zhang, Z.L., 2002. Contamination by polycyclic aromatic hydrocarbons in the Jiulong River estuary and Western Xiamen Sea, China. Environ. Pollut. 118 (1), 109–122.

McRae, C., Sun, C.G., Snape, C.E., Fallick, A.E., Taylor, D., 1999. δ^{13}C values of coal-derived PAHs from different processes and their application to source apportionment. Org. Geochem. 30 (8), 881–889.

Meijer, S.N., Sweetman, A.J., Halsall, C.J., Jones, K.C., 2008. Temporal trends of polycyclic aromatic hydrocarbons in the UK atmosphere: 1991–2005. Environ. Sci. Technol. 42 (9), 3213–3218.

Mitra, S., Bianchi, T.S., Mckee, B.A., Sutula, M., 2002. Black carbon from the Mississippi River: quantities, sources and potential implications for the global carbon cycle. Environ. Sci. Technol. 36, 2296–2302.

Moeckel, C., Monteith, D.T., Llewellyn, N.R., Henrys, P.A., Pereira, M.G., 2013. Relationship between the concentrations of dissolved organic matter and polycyclic aromatic hydrocarbons in a typical UK upland stream. Environ. Sci. Technol. 48 (1), 130–138.

Neff, J., 1979. Polycyclic aromatic hydrocarbons. Sources, fates and biological effects. Applied Science Publ., London, p. 262.

Oen, A.M., Cornelissen, G., Breedveld, G.D., 2006. Relation between PAH and black carbon contents in size fractions of Norwegian harbor sediments. Environ. Pollut. 141 (2), 370–380.

Peters, K.E., Sweeney, R.E., Kaplan, I.R., 1978. Correlation of carbon and nitrogen stable isotopes in sedimentary organic matter. Limnol. Oceanogr. 23, 598–604.

Petrisic, M.G., Muri, G., Ogrinc, N., 2013. Source identification and sedimentary record of polycyclic aromatic hydrocarbons in Lake Bled (NW Slovenia) using stable carbon isotopes. Environ. Sci. Technol. 47 (3), 1280–1286.

Qiao, M., Wang, C.X., Huang, S.B., Wang, D.H., Wang, Z.J., 2006. Composition, sources, and potential toxicological significance of PAHs in the surface sediments of the Meiliang Bay, Taihu Lake, China. Environ. Int. 32, 28–33.

Ramaswamy, V., Gaye, B., Shirodka, P.V., Rao, P.S., Chivas, A.R., Wheeler, D.T.S., 2008. Distribution and sources of organic carbon, nitrogen and their isotopic signatures in sediments from the Ayeyarwady (Irrawaddy) continental shelf, northern Andaman Sea. Mar. Chem. 111, 137–150.

Sánchez-García, L., Cato, I., Gustafsson, Ö., 2010. Evaluation of the influence of black carbon on the distribution of PAHs in sediments from along the entire Swedish continental shelf. Mar. Chem. 119 (1), 44–51.

Sánchez-García, L., Cato, I., Gustafsson, Ö., 2012. The sequestration sink of soot black carbon in the Northern European Shelf sediments. Glob. Biogeochem. Cycles 26 (1), GB1001. http://dx.doi.org/10.1029/2010GB003956.

Sánchez-García, L., de Andrés, J.R., Gélinas, Y., Schmidt, M.W., Louchouarn, P., 2013. Different pools of black carbon in sediments from the Gulf of Cádiz (SW Spain): method comparison and spatial distribution. Mar. Chem. 151, 13–22.

Sarria-Villa, R., Ocampo-Duque, W., Páez, M., Schuhmacher, M., 2016. Presence of PAHs in water and sediments of the Colombian Cauca River during heavy rain episodes, and implications for risk assessment. Sci. Total Environ. 540, 455–465.

Savinov, V.M., Savinova, T.N., Matishov, G.G., Dahle, S., Nae, K., 2003. Polycyclic aromatic hydrocarbons (PAHs) and organochlorines (OCs) in bottom sediments of the Guba Pechenga, Barents Sea, Russia. Sci. Total Environ. 306, 39–56.

Simcik, M.F., Eisenreich, S.J., Lioy, P.J., 1999. Source apportionment and source/sink relationships of PAHs in the coastal atmosphere of Chicago and Lake Michigan. Atmos. Environ. 33 (30), 5071–5079.

Sofowote, U.M., McCarry, B.E., Marvin, C.H., 2008. Source apportionment of PAH in Hamilton Harbor suspended sediments: comparison of two factor analysis methods. Environ. Sci. Technol. 42 (16), 6007–6014.

Song, J.Z., Peng, P.A., Huang, W.L., 2002. Black carbon and kerogen in soils and sediments, 1. Quantification and characterization. Environ. Sci. Technol. 36 (18), 3960–3967.

Sprovieri, M., Feo, M.L., Prevedello, L., Manta, D.S., Sammartino, S., Tamburrino, S., Marsella, E., 2007. Heavy metals, polycyclic aromatic hydrocarbons and polychlorinated biphenyls in surface sediments of the Naples harbour (southern Italy). Chemosphere 67, 998–1009.

US EPA, 1993. Provisional guidance for quantitative risk assessment of polycyclic aromatic hydrocarbons, EPA/600/R-93/089. Office of Research and Development, US Environment Protection Agency, Washington, DC.

US EPA, 1996. Method 3540C, Soxhlet extraction. http://www.epa.gov/osw/hazard/testmethods/sw846/pdfs/3540c.pdf (14.03.14).

US EPA (United States Environmental Protection Agency), 2005. Guidelines for Carcinogen Risk Assessment EPA/630/P-03/001B. Risk Assessment Forum National Center for Environmental Assessment (Washington DC).

Wang, J.Z., Guan, Y.F., Ni, H.G., Luo, X.L., Zeng, E.Y., 2007. Polycyclic aromatic hydrocarbons in riverine runoff of the Pearl River Delta (China): concentrations, fluxes, and fate. Environ. Sci. Technol. 41 (16), 5614–5619.

Wang, Q., Liu, M., Yu, Y.P., Du, F.F., Wang, X., 2014a. Black carbon in soils from different land use areas of Shanghai, China: level, sources and relationship with polycyclic aromatic hydrocarbons. Appl. Geochem. 47, 36–43.

Wang, R., Tao, S., Shen, H., Huang, Y., Chen, H., Balkanski, Y., Boucher, O., Ciais, P., Shen, G.F., Li, W., Zhang, Y.Y., Chen, Y.C., Lin, N., Su, S., Li, B.G., Liu, J.F., Liu, W.X., 2014b. Trend in global black carbon emissions from 1960 to 2007. Environ. Sci. Technol. 48 (12), 6780–6787.

Wiedemeier, D.B., Brodowski, S., Wiesenberg, G.L., 2015. Pyrogenic molecular markers: linking PAH with BPCA analysis. Chemosphere 119, 432–437.

Wu, Y., Eglinton, T., Yang, L., Deng, B., Montluçon, D., Zhang, J., 2013. Spatial variability in the abundance, composition, and age of organic matter in surficial sediments of the East China Sea. J. Geophys. Res. Biogeosci. 118 (4), 1495–1507.

Xing, L., Zhang, H.L., Yuan, Z.N., Sun, Y., Zhao, M.X., 2011. Terrestrial and marine biomarker estimates of organic matter sources and distributions in surface sediments from the East China Sea shelf. Cont. Shelf Res. 31 (10), 1106–1115.

Yuan, D., Yang, D., Wade, T.L., Qian, Y., 2001. Status of persistent organic pollutants in the sediment from several estuaries in China. Environ. Pollut. 114 (1), 101–111.

Yunker, M.B., Snowdon, L.R., Macdonald, R.W., Smith, J.N., Fowler, M.G., Skibo, D.N., McLaughlin, F.A., Danyushevskaya, A.I., Petrova, V.I., Ivanov, G.I., 1996. Polycyclic aromatic hydrocarbon composition and potential sources for sediment samples from the Beaufort and Barents Seas. Environ. Sci. Technol. 30, 1310–1320.

Yunker, M.B., Macdonald, R.W., Vingarzan, R., Mitchell, R.H., Goyette, D., Sylvestre, S., 2002. PAHs in the Fraser River basin: a critical appraisal of PAH ratios as indicators of PAH source and composition. Org. Geochem. 33, 489–515.

Zakaria, M.P., Takada, H., Tsutsumi, S., Ohno, K., Yamada, J., Kouno, E., Kumata, H., 2002. Distribution of polycyclic aromatic hydrocarbons (PAHs) in rivers and estuaries in Malaysia: a widespread input of petrogenic PAHs. Environ. Sci. Technol. 36 (9), 1907–1918.

Zhang, Z.L., Hong, H.S., Zhou, J.L., Yu, G., 2004. Phase association of polycyclic aromatic hydrocarbons in the Minjiang River Estuary, China. Sci. Total Environ. 323 (1), 71–86.

Zhang, Y., Guo, C.S., Xu, J., Tian, Y.Z., Shi, G.L., Feng, Y.C., 2012. Potential source contributions and risk assessment of PAHs in sediments from Taihu Lake, China: comparison of three receptor models. Water Res. 46 (9), 3065–3073.

Zhang, J.D., Wang, Y.S., Cheng, H., Jiang, Z.Y., Sun, C.C., Wu, M.L., 2015. Distribution and sources of the polycyclic aromatic hydrocarbons in the sediments of the Pearl River estuary, China. Ecotoxicology 24 (7–8), 1643–1649.